3rd International Conference on Tomography of Materials and Structures
Lund, Sweden, 26-30 June 2017, ICTMS2017-105

DETECTING FLAWS IN ADDITIVE MANUFACTURING USING X-RAY AND NEUTRON INTERFEROMETRY

Adam J. Brooks*[1], Omoefe Kio[1], Kyungmin Ham[2] & Leslie G. Butler[1]

[1]Department of Chemistry, Louisiana State University, Baton Rouge, LA 70803, USA
[2]Center for Advanced Microstructures and Devices, Louisiana State University, Baton Rouge, LA 70806, USA

Keywords: x-ray and neutron tomography, grating interferometry, additive manufacturing

Summary: X-ray interferometry/tomography of 3D polymer printed samples shows defects between filament layers. Neutron interferometry/tomography of electron beam melted titanium alloy samples discovered structures that initially appear to be low density pores based on attenuation, but have scattering characteristic of phase separation. Fatigued samples are imaged as a function of interferometry tuning to access a range of autocorrelation scattering lengths.

1. INTRODUCTION

X-ray and neutron tomography offer interesting access to flaws---pores, cracks, and phase separations---in additive manufactured (AM) samples [1]. Access to sub-pixel defects is enhanced by interferometry methods [2,3] and leads to a range of applications for materials science [4,5]. Herein, we explore the correlation [6] between two interferometry image modalities, absorption and dark-field (scattering) as an efficient strategy for defect detection and characterization. The underpinning for interpreting the dark-field images comes from the X-ray and neutron scattering community [7].

Recently, we have been comparing two interferometry designs, both based on grating interferometry. Grating interferometry typically uses micron-dimension linear structures fabricated on Si-wafers; the linear structures can be used as either absorption or phase shift material. A Talbot-Lau interferometer is constructed with one phase shift and two absorption gratings and this design accounts for most of the recent X-ray and neutron interferometry publications. A second design, a far-field interferometer [8], can be implemented with one absorption and two phase shift gratings. One advantage of the far-field interferometer is access to a wide range of autocorrelation scattering lengths, nearly two orders of magnitude used in this work. Currently, the Talbot-Lau interferometer is the standard design, but the far-field interferometer is highly recommended for additional evaluation.

2. EXPERIMENTAL METHOD

The experiments were performed at several sites. Talbot-Lau X-ray interferometry was performed at the LSU CAMD and a laboratory X-ray interferometer at LSU. Talbot-Lau neutron interferometry was utilized at the Helmholtz-Zentrum Berlin CONRAD-2 beamline. Two-dimensional, single-shot Talbot X-ray interferometry with a checkerboard phase grating was performed at the Advanced Photon Source 1-BM-B synchrotron beamline. Far-field neutron interferometry was performed at the NIST NG6 beamline.

3. RESULTS

The data processing workflow is evolving into a comparison of absorption and dark-field intensities, either from 2D projections [8] or 3D tomography reconstructions (Fig. 1). The dark-field image contains orientation information [4,5] and we are finding that AM flaw detection often requires two orthogonal setups of the interferometer or sample. The high signal-to-noise absorption (or attenuation) image is used to generate a mask which is then applied to the low S/N dark-field image so as to define a region of interest. Additionally, the mask can also be used to define sample properties such as space plane curvature, a parameter which has been useful to correlate the defects observed between the dark-field image with AM parameters such as printhead trajectory.

* e-mail: author.one@university.edu

References

[1] Thompson, A., Maskery, I., Leach, R.K. X-ray computed tomography for additive manufacturing: a review. *Meas. Sci. Technol*. 27, 7, 2016.
[2] A. Hilger, N. Kardjilov, T. Kandemir, I. Manke, J. Banhart, D. Penumadu, A. Manescu, M. Strobl, Revealing microstructural inhomogeneities with dark-field neutron imaging, *Journal of Applied Physics*, 107, 2010.
[3] T. Lauridsen, M. Willner, M. Bech, F. Pfeiffer, R. Feidenhans'l, Detection of sub-pixel fractures in X-ray dark-field tomography, *Applied Physics a-Materials Science & Processing* 121, 1243-1250, 2015.
[4] V. Revol, C. Kottler, R. Kaufmann, A. Neels, A. Dommann, Orientation-selective X-ray dark field imaging of ordered systems, *Journal of Applied Physics* 112, 2012.
[5] A. Malecki, E. Eggl, F. Schaff, G. Potdevin, T. Baum, E.G. Garcia, J.S. Bauer, F. Pfeiffer, Correlation of X-Ray Dark-Field Radiography to Mechanical Sample Properties, *Microscopy and Microanalysis* 20, 1528-1533, 2014.
[6] H. Wen, E.E. Bennett, M.A. Hegedus, S.C. Carroll, Spatial harmonic imaging of X-ray scattering initial results, *IEEE Transactions on Medical Imaging* 27, 997-1002, 2008.
[7] R. Andersson, L. F. van Heijkamp, I. M. de Schepper, and W. G. Bouwman, Analysis of spin-echo small-angle neutron scattering measurements, *J. Appl. Crystl*. 41, 868-885, 2008.
[8] H.X. Miao, A. Panna, A.A. Gomella, E.E. Bennett, S. Znati, L. Chen, H. Wen, A universal moire effect and application in X-ray phase-contrast imaging, *Nature Physics* 12, 830-834, 2016.

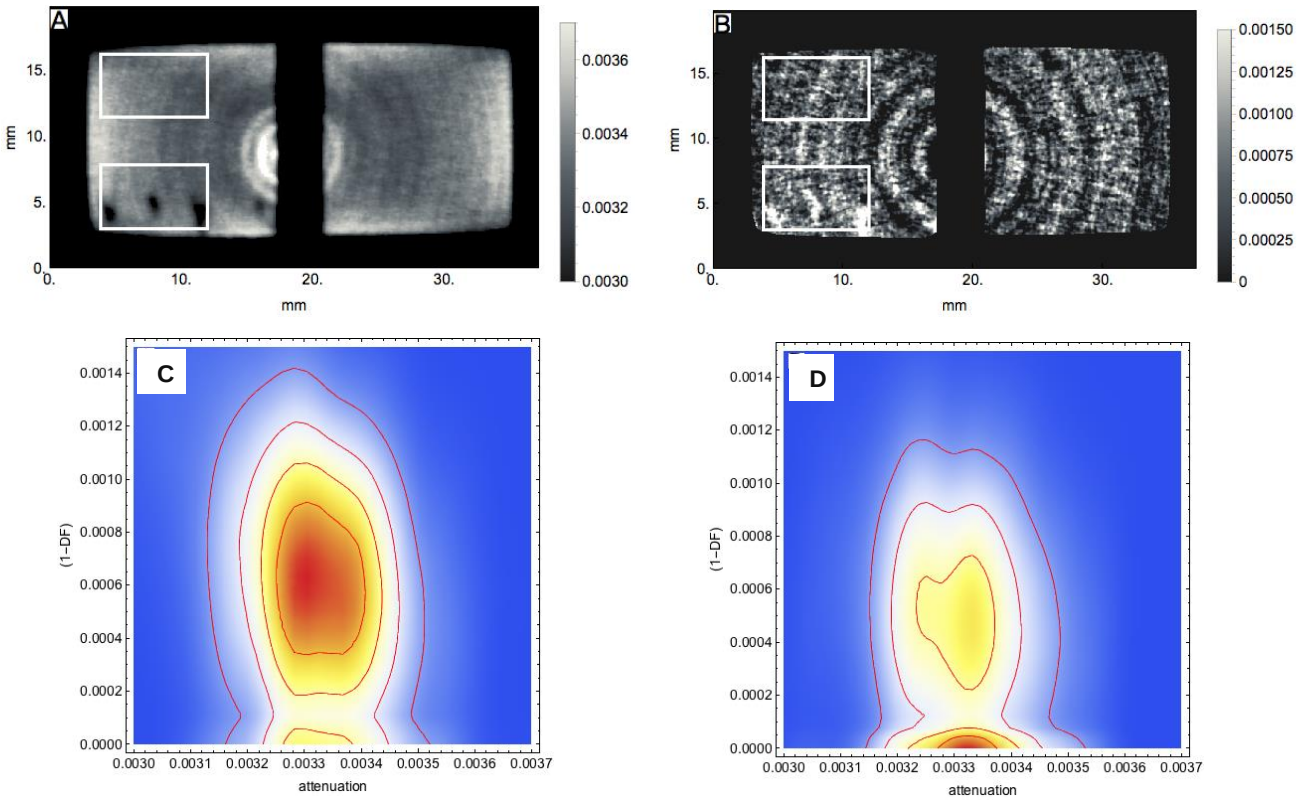

Figure 1: (A) Attenuation and (B) darkfield slices from the grating interferometry attenuation and darkfield volumes of Ti-6Al-4V cubes. The left cube is a 2016 sample and the right cube from 2015. Both the attenuation and dark-field images show the features of interest in the lower portion of the 2016 sample. Histograms of the lower (C) and upper (D) white rectangles shows a wide dispersion of dark field intensities, yet a moderate range of attenuation values, indicating phase separation, not air-filled pores.